Electrical Power and Energy Systems 53 (2013) 733–741

Contents lists available at SciVerse ScienceDirect

Electrical Power and Energy Systems

journal homepage: www.elsevier.com/locate/ijepes

MCHO – A new indicator for insulation conditions in transmission lines

Martin Max L.C. Negrão [a], Paula Renatha N. da Silva [b,*], Cristiane R. Gomes [c], Hermínio S. Gomes [c], Petrônio Vieira Junior [a], Miguel A. Sanz-Bobi [d]

[a] School of Electrical Engineering, Institute of Technology, Federal University of Pará, Avenida Augusto Corrêa, 1, 66075-900 Belém, Brazil
[b] Institute of Engineering and Geosciences, Federal University of West Pará, Rua Vera Paz, S/N, 68035-110 Santarém, Brazil
[c] School of Mathematics, Institute of Exact and Natural Sciences, Federal University of Pará, Avenida Augusto Corrêa, 1, 66075-900 Belém, Brazil
[d] Pontificia Comillas University, ICAI School of Engineering, Institute for Technological Investigation, Alberto Aguilera, 23, 28015 Madrid, Spain

ARTICLE INFO

Article history:
Received 15 December 2012
Received in revised form 30 April 2013
Accepted 29 May 2013

Keywords:
Leakage current
Capacitance
Permittivity
Transmission line
Detection and diagnosis

ABSTRACT

Conventionally monitoring operating conditions of a power transmission line is accomplished by periodic inspections along this line. This monitoring allows corrective maintenance by finding faults during the inspection. But in more efficient maintenance, predictive techniques that are characterized by real-time monitoring should be employed. Such predictive techniques allow for verifying the working status of the line by using normal working models to detect faults and fault models for diagnosis. This paper presents a study that used a mathematical model appropriate for application to predictive maintenance of transmission line segments at low cost, without the need for sensors distributed along the line, and presenting a new indicator of transmission line operation conditions. By tracking the leakage current of transmission lines, this model allows for estimating the current line insulation status. Once the current line insulation status is known, it is possible to compare it against other future status and verify the progress of the insulation conditions of that line. The model uses a new indicator, called MCHO, which can detect and diagnose both normal and abnormal operating conditions of a power transmission line. This new indicator is the capacitance of the harmonic frequencies of the transmission line leakage current. The model was validated through measurements obtained on a stretch of transmission line.

1. Introduction

The pollution from insulators, vandalism, fires, urban encroachment by building on the right of way of the line can cause faults and resultant outages in transmission lines (TLs). These events can reduce the level of isolation of the line, causing an increase in its leakage current (I_L). The evolution of these events is gradual, which presumes the possibility of observing these developments up until the occurrence of the fault. Added to these events has been the phenomenon of aging and natural wear of the line that must be considered when checking the level of isolation thereof. There are methods for real-time detection of faults in TLs, some analyze the line voltage and current, observing the phase between them for locating faults [1]. Other methodologies analyze the characteristics of voltage and current phasors to estimate the state of the transmission lines [2,22]. There are some methods that analyze temporal samples of the voltage and current for measuring the impedance of the transmission line and allow the use of systems for estimating the location of faults [3]. These methods, however, do not have the power to estimate the state of insulation of the transmission line nor predict a fault. On the other hand, work such as that of [4] observed the change in the behavior of I_L in the occurrence of flashover. Other works such as [5,6], found that through the harmonic decomposition of the leakage current in contaminated insulators, there is a maximum level of magnitude for certain frequencies, and they signal the malfunction of the insulation. Kanashiro (1996) [7]included in his article the climatic effects added to marine and industrial pollution. In these latest studies it has been found that monitoring the insulation or operating conditions of a TL may be performed through observation of the I_L current. This paper uses this finding to develop models to be employed in the detection and diagnosis, thus, to allow for developing a predictive and automatic protection methodology in TLs. This article presents a proper model aimed at the detection and diagnosis of fauls in TL by analyzing the I_L. Through this model, a new indicator of the state of operation of TL's, able to characterize

☆ Thanks to Eletronorte for funding through the On-line Monitoring Project for transmission lines, from which all actual data analyzed in this study were collected.
* Corresponding author. Tel.: +55 093 92024637; fax: +55 093 21014956.
E-mail address: paularenatha@hotmail.com (P.R.N.DA Silva).

0142-0615
http://dx.doi.org/10.1016/j.ijepes.2013.05.052

their normal operation and failure modes, is proposed. Another aspect that is influenced by natural wear of a TL is its load carrying capacity and therefore the financial return it can offer. Currently this TL wear is estimated. With the characterization of the operating conditions of the power line, real wear can be considered in calculating the financial return of a TL.

2. Development of an adequate detection and diagnosis model

The methods for fault detection applied to continuous monitoring and associated with time, enable developing methods to predict faults [8,9]. The detection of faults for prediction should compare, continuously and in real time, the normal system behavior with actual behavior, as suggested by Fig. 1. The signal resulting from this comparison is called a residual. For diagnosis, signal patterns of failure modes and the signals of the residual can be used, as suggested by Fig. 1.

To use this methodology, the use of normal operation and failure mode models is necessary.

2.1. Models for detection and diagnosis problems

The model to be obtained through the studies presented in this article, is to be employed in the detection of incipient fault by model-based method. This method is based on parametric or non-parametric analytical models, with a precision which allowed performing an analytical redundancy [10]. According to [12] the analytical redundancy is based on the comparison between actual measurements and signals generated by a mathematical model of the system. The analytical model of the behavior of failure modes for the inputs of the system and the fault detection and diagnosis is performed by checking the residual, as shown in Fig. 2. The residual is the difference found between the actual measurements and those calculated by the model [11]. A significant residual does not always represents a failure, it might be unexpected behavior which can be described by correlating the model parameters. If this correlation is lost, then it is because a new element was introduced into the system.

Obtaining the residual is the first step for detecting a failure. A second step is to check whether or not this residual represents a failure. In the second step, the information from the residual can have a signature representing a pattern associating the residual signal with the cause of the fault and its location. From the foregoing, one can see the great importance of having a mathematical model of normal operation representing the system analyzed with a high degree of accuracy.

2.2. Identification of the signal for obtaining the residual in detection and diagnosis problems applied to TL's

It was described in the introduction that monitoring the insulation of operating conditions of a TL can be performed by observing the I_L. Moreover, according to [13], the capacitance associated with a resistance represents the TL dielectric losses, i.e. losses represented by I_L, since it normally passes through the insulators. In other words, the behavior of I_L is directly linked to the value of the capacitance of the line. In the detection of faults in transmission lines proposed in this paper, the residual is the result of the comparison of the measured I_L signal with the I_L signal obtained by the mathematical model of normal TL operation. This comparison allows for detection. The diagnosis can be obtained through the comparison against the fault models. On the other hand, the capacitance of a TL varies with environmental variables (EV's) and hence the behavior of I_L as well. Therefore, for the development of the mathematical model of normal LT is necessary to characterize the I_L also in relation to the EV's (temperature, relative humidity). This paper does not develop detection and diagnosis. It presents a promising detection and diagnosis tool.

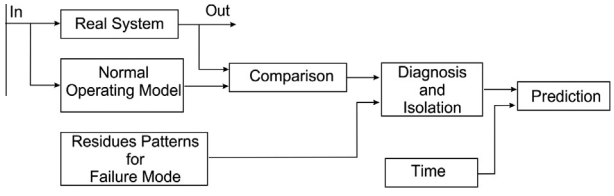

Fig. 1. Fault detection method using a normal operation model and the system fault modes.

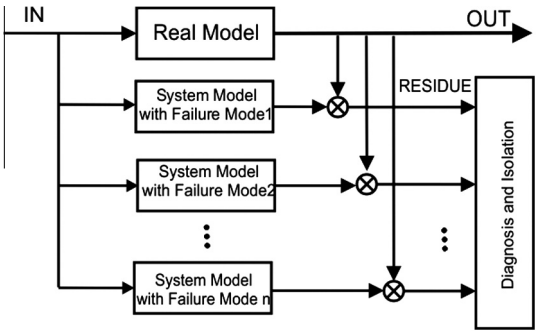

Fig. 2. Method of detection and diagnosis with residuals generated by dynamic models of fault modes.

2.3. Characterization of I_L

The experimental determination of I_L is calculated using the theory of Gaussian surfaces. This theory holds that the algebraic sum of the current entering and leaving a closed surface is equal to zero [14]. On a TL section, this theory applies as shown in Fig. 3. This means that when monitoring a stretch of TL, its I_L can be obtained from the vector sum of the output and input currents of this stretch.

$$I_L = I_{Guamá_{SS}} - I_{Utinga_{SS}} \quad (1)$$

In the literature, some methodologies are presented to determine the I_L in insulators or lightning arresters. However, cannot be found concerning the determination of I_L in a section of TL [21,23,24].

For monitoring of electrical and environmental variables, power analyzer and Remote Weather Station (RWS) was installed at each end of the monitored TL. The measurements performed by the analyzers are synchronized via GPS and every second. The RWS measurements are performed every 20 min. All these equipments are connected to the intranet of the company responsible for that section of the monitored TL. The database is built in real time with the aid of a personal computer (as shown in Fig. 4), equipped with a Core2Quad 2.0 GHz processor with 2 Gb RAM memory. The processing time for determining the I_L measured in the TL and the I_L calculated by the model is approximately 2 min and 10 s.

2.4. Capacitance and EV's – Experiment

The EV's that most influence the capacitance of the TL are: Temperature (T_{amb}), relative humidity (U_{air}) and wind speed (S_{wind}). To investigate the behavior of the capacitance with environmental variation, an experimental bench was constructed. A photographic record of this bench is shown in Fig. 5, whose schematic diagram is shown in Fig. 5.

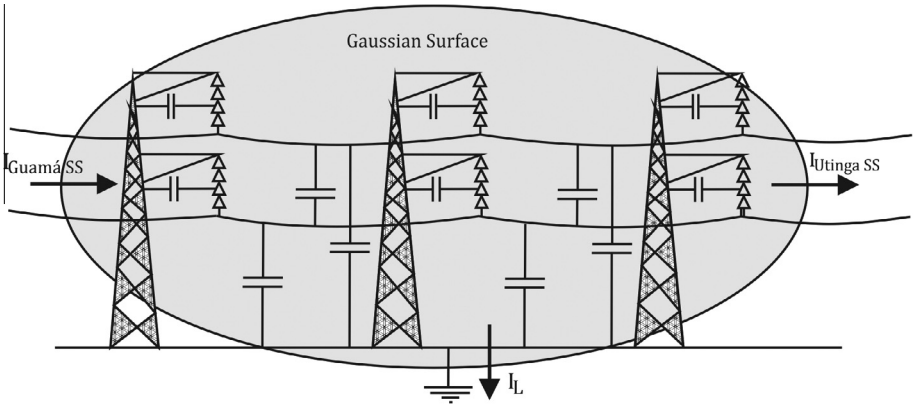

Fig. 3. Application of Gauss' theorem for closed surfaces for a stretch of transmission line.

Fig. 4. Maintenance room for the transmission line, where the data collected from the power analyzers and RWS is gathered.

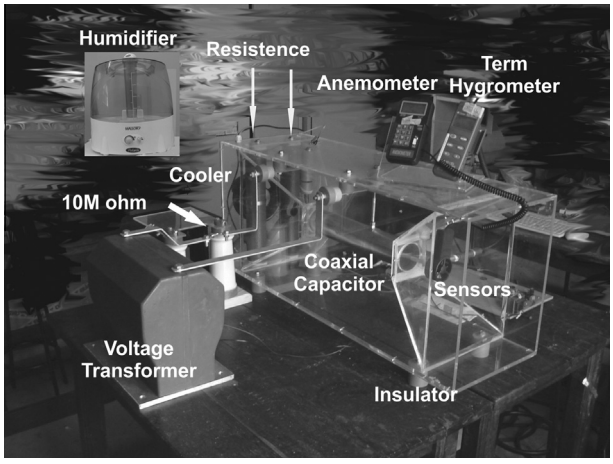

Fig. 5. Test cube.

This bench consists basically of a coaxial capacitor (C) whose capacitance is connected in series with a resistance (R). The coaxial capacitor is installed in a cube of acrylic, called the test cube, where the environmental conditions (ambient temperature, relative humidity and wind velocity) are controlled. According to the diagram (Fig. 6), the current through the capacitor is measured indirectly by reading the voltage V_2 at the terminals of the resistor R. Measurements are performed for various voltage levels and different conditions for U_{air}, T_{amb} and S_{wind}. Temperatures T_{amb1} and T_{amb2}

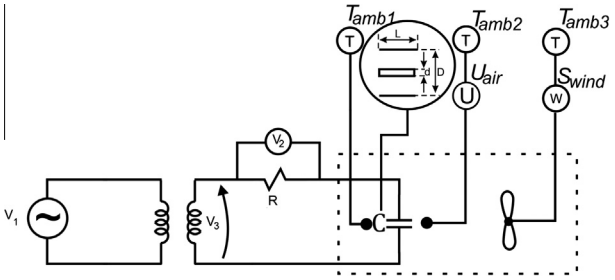

Fig. 6. Electrical schematic of the test cube for determination of the permittivity.

are measured at the input and output of the coaxial capacitor. The temperature T_{amb3} is taken together with the measurement of wind speed S_{wind}.

The tests were guided, maintaining two environmental variables fixed and systematically varying the remaining EV. This is for various voltage levels V_3. The temperature intervals were approximately 35–50 °C. The interval for relative humidity was 50–90%. The voltage levels were 600 V–10 kV. The tests were grouped in spreadsheets that served to look into capacitance behavior in relation to the EVs. The behavior of the environmental variable wind speed is constant with respect to the capacitance and hence was not considered in the modeling. Therefore, the EV's employed were only T_{amb} and U_{air}. These results are consistent with the work of [18], which determined the relationship of the Corona effect with T_{amb} and U_{air}, and [15,16] who investigated the effects of U_{ar} in I_L in TL's. The behavior of the capacitance with variation in temperature, relative humidity and voltage can be observed in Figs. 7 and 8. It is possible to approximate the curves displayed in the figures by second order polynomials for the capacitance behavior in relation to the environmental variables temperature and relative humidity.

2.5. Extrapolation of the capacitance for the voltage levels of the TL

Through numerical extrapolation, the capacitance values with respect to the EV's for up to 230 kV (voltage level of the stretch of TL analyzed) were obtained. This is how the graphs shown in Figs. 9 and 10 were obtained, together with the Eqs. (2) and (3) regarding the capacitance as a function of T_{amb} and capacitance as a function of U_{air}, respectively.

$$C(T_{amb}) = 8.9042 \times 10^{-12} T_{amb}^2 - 4.4181 \times 10^{-10} T_{amb} + 1.5693 \times 10^{-8} \quad (2)$$

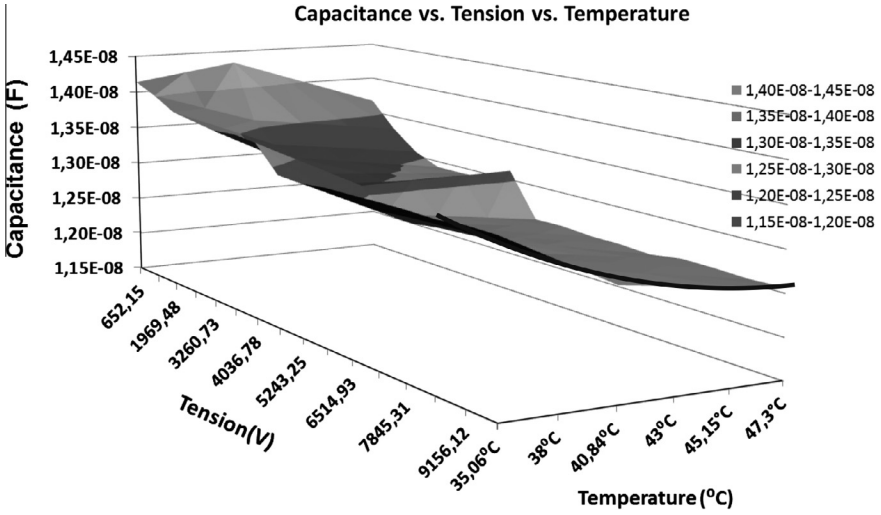

Fig. 7. Behavior of the capacitance with ambient temperature and voltage, with a linear approximation by a second order polynomial.

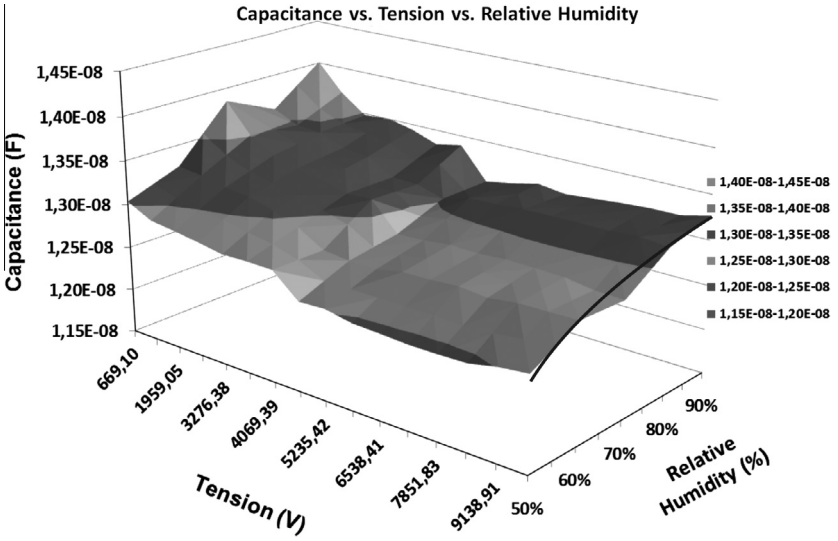

Fig. 8. Behavior of the capacitance with relative humidity and voltage, with a linear approximation by a second order polynomial.

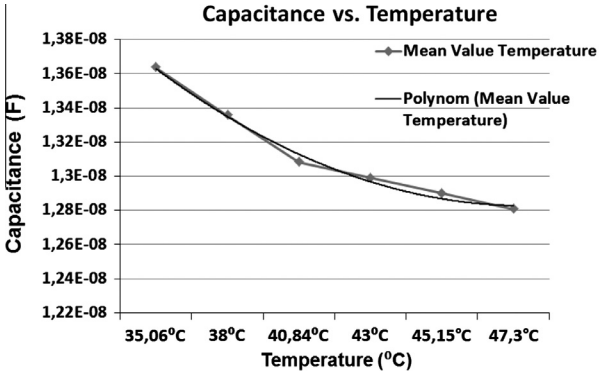

Fig. 9. Behavior of the capacitance in relation to temperature, determined through extrapolation of data.

In which $C(T_{amb})$ – is the capacitance as a function of temperature.

$$C(U_{air}) = 8.3261 \times 10^{-13} U_{air}^2 - 1.4097 \times 10^{-10} U_{air} + 1.6145 \times 10^{-8} \quad (3)$$

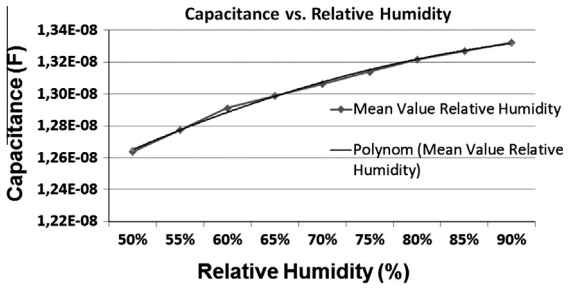

Fig. 10. Behavior of the capacitance in relation to relative humidity, determined through extrapolation of the data.

In which $C(U_{air})$ – capacitance as a function of humidity.

As the mathematical model allows only one equation that considers the effects on capacitance relative to EV's. Eq. (4) has been developed that includes the effects of both EV's simultaneously in the capacitance.

$$C(U_{air}, T_{amb}) = \propto C(T_{amb}) + \beta C(U_{air}) \quad (4)$$

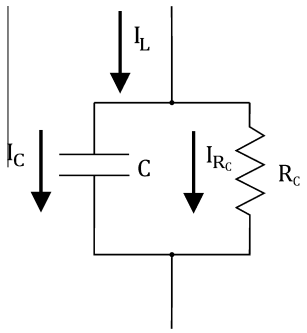

Fig. 11. Insulation schematic.

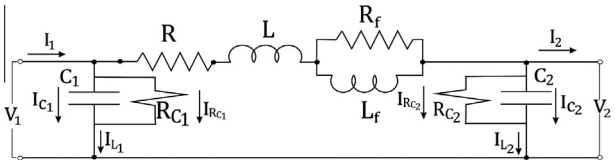

Fig. 12. Equivalent electrical circuit for the mathematical model adopted.

In which $C(U_{air}, T_{amb})$ – capacitance as a function of Humidity and Temperature, $\propto$ – adjustment constant corresponding to temperature, β – adjustment constant corresponding to humidity.

The constants α and β were arbitrarily determined in order to fit better by approximating the capacitance value measured by the test cube, in this way the values of α and β obtained are 0.5076 and 0.5093 respectively, from which Eq. (5) can be written.

$$C(T_{amb}, U_{air}) = 0.5076 \cdot (8.9042 \times 10^{-12} T_{amb}^2 - 4.4181 \times 10^{-10} T_{amb} + 1.5693 \times 10^{-8}) + 0.5093 \cdot (8.3261 \times 10^{-13} U_{air}^2 - 1.4097 \times 10^{-10} U_{air} + 1.6145 \times 10^{-8}) \quad (5)$$

2.6. Determination of the values for the parameters R, L and C of the mathematical model

The model was based on data the constructive from the three-phase Guamá–Utinga TL (between the Guamá substation and the Utinga substation), located in the Amazon region of Brazil, operating at 230 kV, with an approximate length of 20 km and containing 50 towers. The matrix method [13] was used to calculate the parameters *R*, *L*, *C*. The calculation of these parameters for the TL studied can be seen in [17] where it was obtained:

$$R = 1.0955\ \Omega \quad L = 0.07525\ \text{H} \quad C = 116,767\ \text{nF}$$

2.7. Mathematical model of the TL is an equivalent electrical circuit

The insulation of a TL can be characterized by a combination of resistance and capacitance, which can be called capacitance of insulation, as in Fig. 11. The I_L of TL's travels this combination. So the I_L depends on the state of the line insulation.

In this case the I_L is the contribution of the current crossing the insulator (I_C) and the current passing along the surface of the insulator (I_{RC}), namely:

$$I_L = I_C + I_{R_C} \quad (6)$$

The mathematical model of Gary and Skilling-Umoto [20], shown in Fig. 12, is employed to represent the TL, where the TL insulation was shown in Fig. 10. The detection and diagnosis of incipient faults in the insulation of TL's are checked at frequencies between 120 Hz and 3 kHz, so despite the model presented, incorporating this Corona effect will not be checked because it is perceived at frequencies between 2 MHz and 20 MHz [18,19].

The mathematical model in blocks by the tool Simulink/Matlab, is represented in Fig. 13, where each block represents a tower. This configuration, which employs several towers, allows for locating the fault in the TL [21].

The models found in the literature are not used in the detection and diagnosis of transmission lines; for that reason, it is not possible to compare the results.

The capacitance parameter was determined considering the effects of soil and grounding as described in [17]. The capacitance

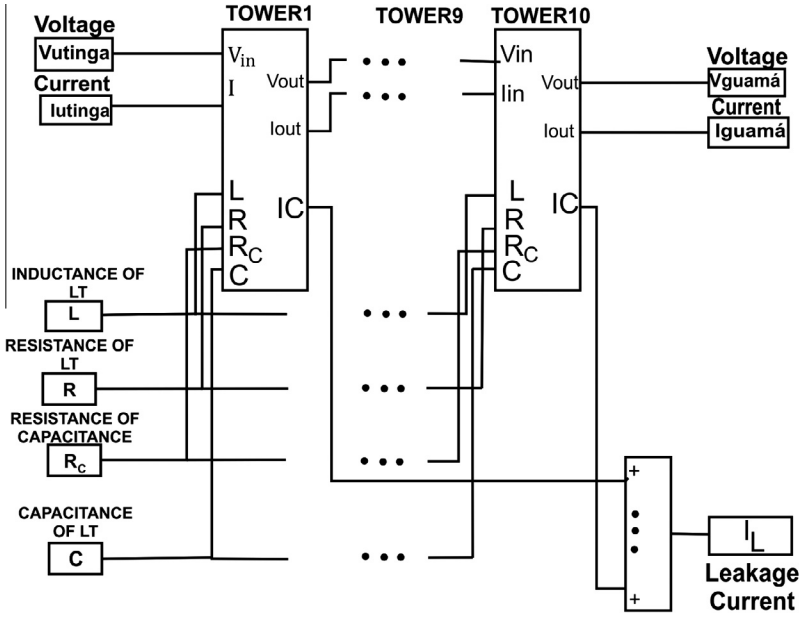

Fig. 13. Mathematical model used for representing the TL done in Simulink/Matlab.

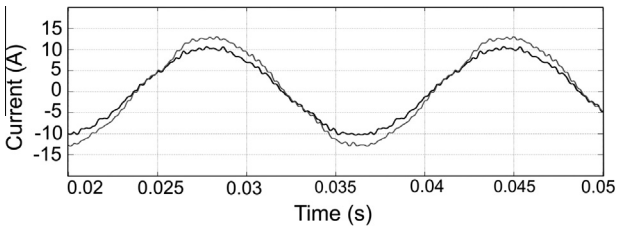

Fig. 14. Superposition of the waveforms of the measurement (black) and calculated by the mathematical model (grey).

values of the model are in terms of the EV's according to their verification below (Eqs. (7) and (8)). This value has been adjusted to incorporate the influences of EV's.

$$I_{C2} = C_2(T_{amb}, U_{air})\frac{dV_2}{dt} \tag{7}$$

$$I_{C1} = C_1(T_{amb}, U_{air})\frac{dV_1}{dt} \tag{8}$$

2.8. Resultados de Simulação simulation results

The curves shown in Figs. 14 and 15 describe the behavior of I_L without considering the EV's. To facilitate visualization, only one of the three phases of the TL is shown. Fig. 14 shows the overlap between the waveforms of I_L measured, in black, and calculated by the model, in grey.

There was a large difference found in the peak value of I_L of approximately 6 A. Using the Mean Squared Error (MSE) it has an error of approximately 0.8.

Fig. 15 represents the decompositions of harmonic components (HDC) of I_L measured (black) and calculated by the model (grey).

It was found that the difference in magnitudes of all frequencies was approximately 0.1, which represents a large error. The improved approximation between the curve obtained by measurement and that obtained by the model is achieved when introducing the EV's. This introduction of the EV's into model can be seen in the block diagram of the simulation, shown in Fig. 16, by inclusion of the blocks T_{amb} and U_{air} and making the block of the insulation capacitance a function of the environmental variables, $C(U_{air}, T_{amb})$ responsible for correlating EV's and Capacitance.

Considering the adjustment of the capacitance as a function of the EV's, a MSE close to 0.05 (see Fig. 17) was obtained. A decrease in the value of Total Harmonic Distortion (THD) as shown in Fig. 17 was also observed.

In Fig. 18 we can see the HDC of I_L measured (black) and I_L calculated by the mathematical model (grey), taking into account the environmental effects of T_{amb} and U_{air}.

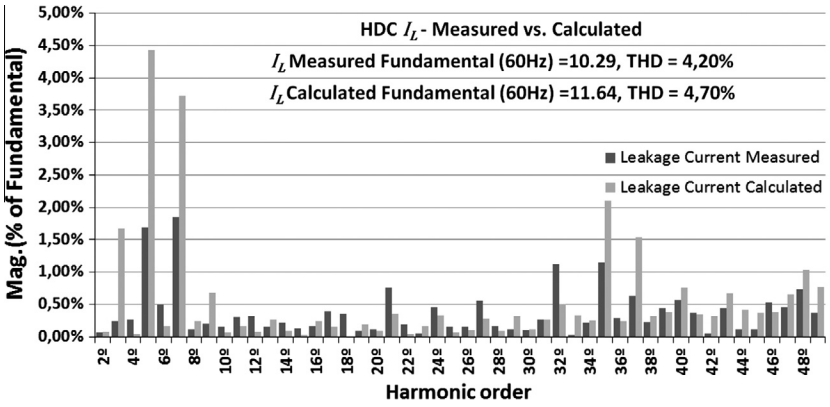

Fig. 15. Harmonic decomposition of the I_L measurement (black) by the instruments installed in the Substations and the I_L calculated (grey) by mathematical model.

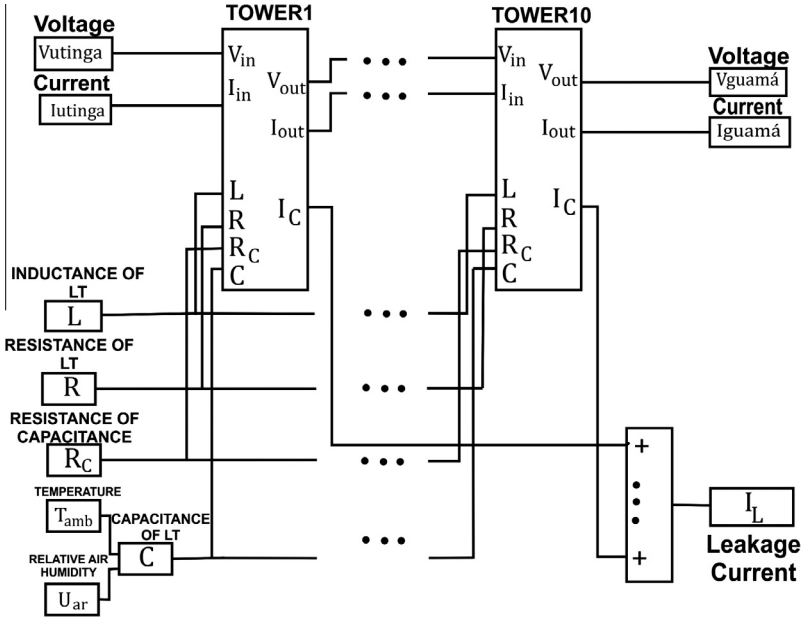

Fig. 16. Mathematical model used to represent the TL, considering the environmental effects, done in Simulink/Matlab.

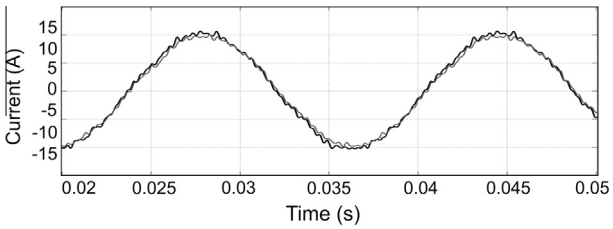

Fig. 17. Superposition of the waveforms of the I_L measurement (black) and calculated by the mathematical model (grey).

Despite improvement in the waveform, the magnitudes of the HDC changed little, maintaining a large error, around 0.1. Signaling for a specific study of the EV's in the frequency domain.

2.9. Detection and diagnosis

One reason for the big difference between the measured and calculated magnitudes of the HDC of I_L are probably that the influences of the EV's are different for each harmonic [15]. PCA was used to obtain the magnitude of these influences for each harmonic. This simple multivariable statistical method can be used for data compression and dimensionality reduction, feature extraction and data projection. In this article it was used in determining which harmonics are more affected by temperature and relative humidity.

Fig. 19 shows the contribution of each harmonic of I_L to temperature variation.

It can be seen that up to the 23rd harmonic there is 96.7% of the complete information, i.e. these are the harmonics that contribute

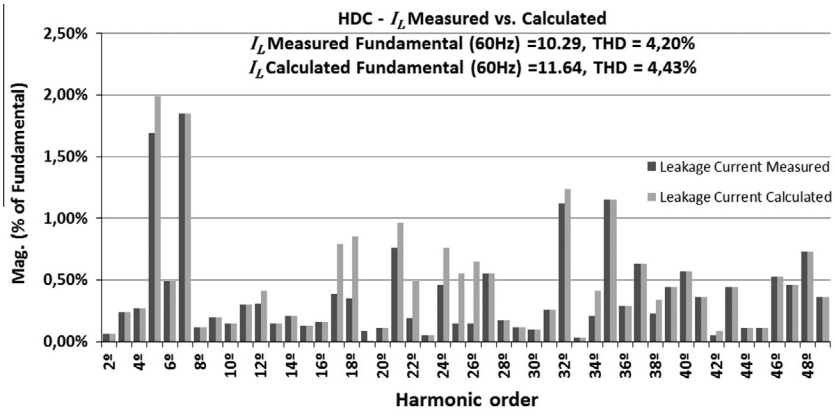

Fig. 18. Harmonic decomposition of the I_L measurement (black) by the instruments installed in the Substations and the I_L calculated by the mathematical model after the first adjustment in the capacitance.

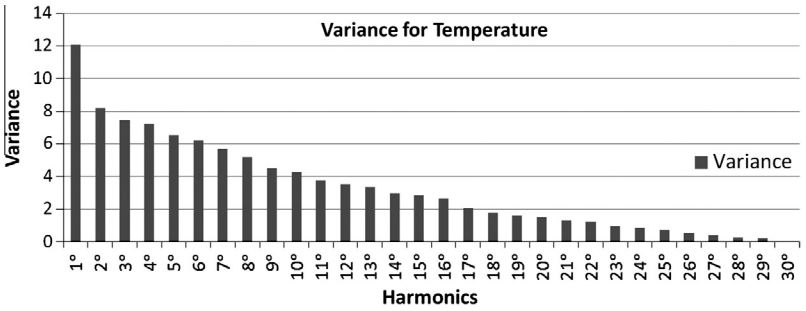

Fig. 19. Ambient temperature contribution for each harmonic of the HDC of the I_L.

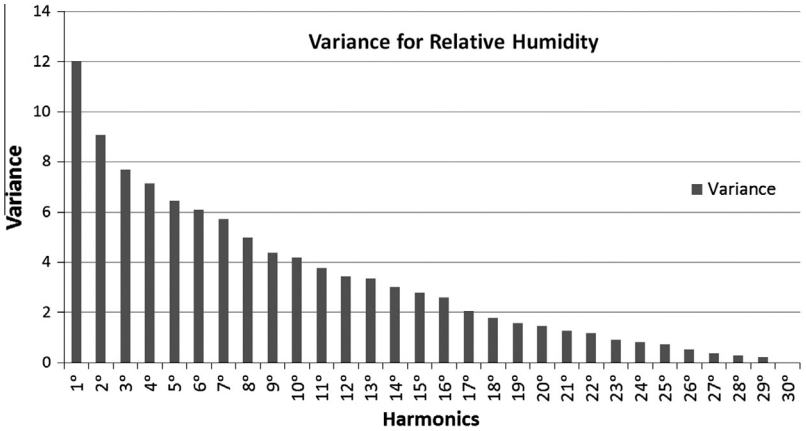

Fig. 20. Relative humidity contribution for each harmonic of the HDC of the I_L.

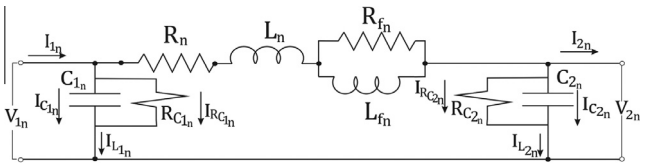

Fig. 21. Electrical circuit diagram used for adjustment of the insulation capacitance due to the VA's through the individual contribution of each harmonic in the I_L.

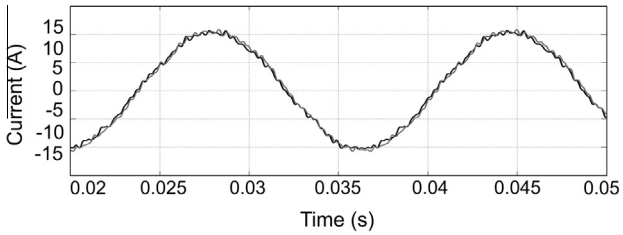

Fig. 22. Superposition of the waveforms of the I_L measured (black) and calculated by the mathematical model (grey), with adjustment of the insulation capacitance due to the VA's and individual contribution of each harmonic in the I_L.

most to the value of capacitance due to temperature variation. Fig. 20 is the distribution of each harmonic of I_L for variation in relative humidity.

After determination of the magnitudes that each harmonic of the HDC of the I_L has due to the EV's, these results are used in the model by applying the superposition theorem. This Theorem allows for defining a model whereby each nth frequency (n) of each harmonic contributes as an individual electrical circuit (n), as shown in Fig. 21. The result, considering all the harmonics simultaneously, is obtained through the sum of each individual contribution.

In Fig. 22, the waveforms of I_L obtained from measurements (black) and the mathematical model (grey) can be seen, with insulation capacitance individually adjusted for each frequency, taking the EV's into account. In this figure the MSE was around 0.02, thus an error much smaller than the previously presented.

Fig. 23 shows the harmonic decomposition of the I_L measured (black) and I_L calculated by the mathematical model (grey), with the insulation capacitance value individually adjusted for each frequency taking the EV's into account. This MSE was around 0.009.

It can be observed that the detection model succeeds in reproducing both the waveform and the harmonic decomposition of with a good degree of fidelity. Through this methodology it is possible to reproduce the waveform of I_L by the mathematical model with an acceptable degree of accuracy for detection of incipient faults. Where the determination of the model of normal operation must be obtained is through characterizing the operating state at the time capacitance adjustments were characterized for a given moment in the monitoring of the line. Therefore the model of normal operation should evolve according to the operating status of the TL. Thus this methodology allows verifying the degradation of the line in its normal operating state. So this model also suggests a methodology for evaluating the efficiency of the line based on its natural degradation and not the conditions at the time of its installation and design data. Finally, adjustment of the capacitance for each harmonic frequency suggests that this is the identifier of disturbances in the TL. In other words, this adjustment could diagnose the cause of the incipient failure. With this, a new indicator of the conditions of isolation that LT can be suggested, which is the magnitude of the capacitance of the line in adjusting the leakage current for each harmonic order, known in this article as MCHO (Magnitude of the Capacitance by Harmonic Order). The validation of the finding of this new indicator is the subject of research still in progress.

3. Conclusion

This study found that environmental variables influence specific harmonics of the transmission line leakage current from the experimental verification of the correlation between capacitance and environmental variables. The transmission line model used was that of Gary and Skilling-Umoto who obtained good results for fault detection for capacitance values dependent on the environmental variations. The model is dynamic, since operating conditions vary with the degradation of the insulation. That is, the normal operating model of a TL evolves with time due to natural wear. This model is suitable to the methodology for the detection and diagnosis of incipient faults in a transmission line that seeks the identification of a normal model at a particular instant. That is, this model allows checking when a fault condition becomes a normal condition due to natural wear in the transmission line. This reasoning can be extended to the failure mode models to be used in diagnosis. This model has, as a key advantage, continuous monitoring that seeks the indication of normal operation and the failure modes considering the natural wear on the TL, and thus characterizing the conditions in which this line can be operated, contributing to the determination of the real remuneration of the transmission line. Finally this paper contributes by suggesting a new indicator of the conditions of the TL insulation, which is the magnitude of the capacitance of the line in adjusting the leakage

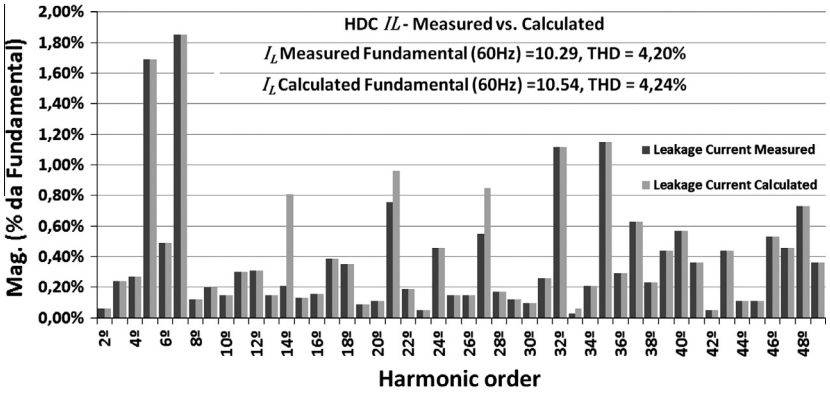

Fig. 23. Harmonic decomposition of the I_L calculated by the mathematical model, with adjustment of the insulation capacitance due to the VA's and individual contribution of each harmonic in the I_L.

current for each harmonic order, referred to in this article as MCHO (Magnitude of the Capacitance by Harmonic Order).

References

[1] Graeme Heggie. Detection de Defaillance Dans Les Lignes de Transport D'electricite. (Patente) ALSTOM UK LTD. CA2314838; 2001.

[2] Zima M, Rehtanz C. Electric power transmission network state estimation. (Patente) ABB RESEARCH LTD. [Affolternstrasse 52, 8050 Zürich, CH] EP1324455; 2005.

[3] Bachmann Bernhard. Impedance measurement system for power system transmission lines. (Patente) ABB Inc. US6397156; 2002.

[4] Suda T. Frequency characteristics of leakage current waveforms of an artificially polluted suspension insulator. IEEE Trans Dielectrics Electr Insul 2001;8(4). p. 705 a 709.

[5] Zhicheng G, Guoshun C. A study on the leakage current along the Surface of Polluted Insulator. In: Proceedings of the 41th international conference on hpenies and Apphcatlons of Dlelectnc materials. Brisbane Australia. Paper 5110; July 3–8, 1994.

[6] Douar MA, Mekhaldi A, Bouzidi MC. Frequency analysis of the leakage current under non uniform polluted conditions on one insulator plane model. Annual report conference on electrical insulation and dielectric phenomena. 978–1-4244-9470-5/10 IEEE; 2010.

[7] Kanashiro AG, Burani GF. Leakage current monitoring of insulators exposed to marine and industrial pollution. Conference record of the 1996 IEEE international symposium on electrical insulation, Montreal, Quebec, Canada; June 16–19, 1996. 271 p.

[8] Isermann R. Fault-diagnosis system: an introduction from fault detectionto fault tolerance. Springer; 2005.

[9] Fernández MCG. Planificacion y Medida de la Efectividade del Mantenimiento Predictivo Aplicado a um Processo Industrial Basándose em el Uso de Técnicas de Modelado de su Comportamiento y de Inteligencia Artificial. Tesis Dep. De Eletrónica y Automatica, Escuela Técnica Superior de Ingeniaría (ICAI), Universidad Pontificia Comillas de Madrid, Madrid; 2004.

[10] Randall RB. Detection and diagnosis of incipient bearing failure in helicopter gearboxes. Eng Fail Anal 2004;11(2):177–90.

[11] Simani S, Fantuzzi C. Dynamicsystem identification and model-based faultdiagnosis of an industrial gas turbine pro-totype. Mechatronics 2006;16:341{363}.

[12] Simani S, Fantuzzi C. Neural networks for fault diagnosis and identification of industrial processes. In: ESANN, editor. ESANN'02 Proc. of the 10th European symposium on artificial, neural networks, vol. 1. Bruges, Belgium; April, 24–26 2002. p. 489–94.

[13] Fuchs RD. Transmissão de Energia Elétrica: Linhas Aéreas. 2ª Edição. Rio de Janeiro: Livros Técnicos e Científicos; 1979.

[14] Butkov E. Matematical physics. St. Jonh's University: New York. Addison-Weslley Publishing Company. 420 p.

[15] Li JY, Sun CX, Sebo SA. Humidity and contamination severity impact on the leakage currents of porcelain. Published in IET generation, transmission & distribution, vol. 5, no. 1. Received on 6th October 2009.Revised on 12th July 2010. Distrib.; 2011. p. 19–28.

[16] Mao Y, Zincheng G, Wang L. Analysis of the leakage current pulses of outdoor insulators in different relative humidity. Annual report conference on electrical insulation and dielectric phenomena; 2007. p. 400 a 403.

[17] Vieira P Jr., Gomes CR, Côrrea, S. M., Gomes Jr., L. A. "Computation of Capacitance of a Transmission Line using the Finite Element Method", In: International Conference on Condition Monitoring and Diagnosis – CMD, Changwon, 2006.

[18] Wei-Gang H. Computation of electro-magnetic transients on three-phase transmission lines with corona and frequency dependent. IEEE Trans Power Deliv 1987;PWRD-2(3):887–98.

[19] Wang W, Chengrong L, Jianbing F, Chen G, Jun Z, Yitao J. The effect of temperature and humidity on corona performance of UHV DC transmission line. Electrical insulation. ISEI 2008. Conference record of the 2008 IEEE International symposium on; 2008.

[20] Mamis MS. State-space transient analysis of single-phase transmission lines with corona. International conference on power systems transients (IPST' 2003), New Orleans; 2003.

[21] Silva PRN, Negrão MMLC, Vieira Junior P, Sanz-Bobi MA. A new methodology of fault location for predictive maintenance of transmission lines. Int J Electr Power Energy Syst 2012;42(1):568–74.

[22] Jiang Z, Miao S, Xu H, Liu P, Zhang B. An effective fault location technique for transmission grids using phasor measurement units. Int J Electr Power Energy Syst 2012;42(1):653–60.

[23] Bakar AHA, Talib DNA, Mokhlis H, Illias HA. Lightning back flashover double circuit tripping pattern of 132 kV lines in Malaysia. Int J Electr Power Energy Syst 2013;45(1):235–41.

[24] Stojanović Zoran N, Stojković Zlatan M. Evaluation of MOSA condition using leakage current method. Int J Electr Power Energy Syst 2013;52:87–95.